Grain growth behavior, surface morphology evolution, structures, and optical properties of ZnO thin films prepared by RF reactive magnetron sputtering

HUI LU[a*], ZHI-JIA ZHENG[a], XIAN LIN[b], FEI XU[a], HAN BI[a], AATTO LAAKSONEN[c]
[a]*Department of Physics, East China University of Science and Technology, Shanghai 200237, China*
[b]*Department of Physics, Shanghai University, Shanghai 200444, China*
[c]*Division of Physical Chemistry, Department of Materials and Environmental Chemistry, Stockholm University, S-10691 Stockholm, Sweden*

ZnO thin films were prepared by radio frequency (RF) reactive magnetron sputtering at varying deposition conditions. The effects of RF power (from 40 to 90 W) and substrate temperature (from 100 to 200 ℃) on the grain growth behavior, surface morphology evolution, and the structural and optical properties of the films were investigated. Atomic force microscopy (AFM) measurements confirmed that the grain size and surface roughness depend mainly on the RF power and increase with increasing it at the initial deposition stage of 5 s, and are strongly affected by the substrate temperature and increase with increasing it at the final deposition stage of 45 min. The influence of both the deposition parameters on the surface structure of the ZnO films at different deposition stages and the mechanism concerning this influence were discussed. The X-ray diffraction (XRD) and optical absorption spectra analysis indicated that all the films deposited for 45 min are in the state of the compressive stress and exhibit polycrystalline nature with the (002) preferential orientation, and they have high optical transparency in the visible range and sharp absorption edges around the wavelength 360 nm corresponding to the ZnO exciton. With the increase of the RF power and substrate temperature, the grain size increases, the residual compressive stress relaxes, and the optical band gaps broaden. In comparison with the RF power, the substrate temperature has more evident influence on the microstructure of the ZnO thin films.

(Received September 17, 2012; accepted January 22, 2014)

Keywords: ZnO Thin films, RF magnetron sputtering, Deposition, Microstructure, Optical properties

1. Introduction

Great attention has been paid to zinc oxide (ZnO) thin films due to their potential for applications in light emitting devices [1,2], transparent conductors [3], surface acoustic wave devices [4], varistors [5], gas sensors [6], etc. The electrical and optical properties of ZnO thin films are closely related to the behavior of crystal grain growth and microstructure of the films, which depend greatly on the deposition methods and parameters. Several techniques have been used for the fabrication of ZnO thin films, including chemical vapor deposition (CVD) [7], molecular beam epitaxy (MBE) [8], pulsed laser deposition [9], and the sol-gel technique [10]. Due to its great flexibility in controlling the film composition and structure as well as the allowance of the film deposition at low temperatures, magnetron sputtering has become widely employed [11]. A detailed and systematic investigation on the influence of sputtering conditions on the microstructure of films is of great importance for better understanding of different factors controlling the film structure, improvement of the film growth and quality, as well as fabrication of ZnO based film devices [12-15].

In this paper, we report the structural and optical properties of the ZnO thin films deposited by radio frequency (RF) reactive magnetron sputtering at different substrate temperatures and RF powers. The behavior of the grain growth and the evolution of the surface morphology of ZnO films under different sputtering conditions are discussed in detail.

2. Experimental procedure

ZnO thin films were deposited on glass substrates by an RF reactive magnetron sputtering system (JCP-200). A 4 mm thick disc of Zinc with a diameter of 50 mm and purity of 99.99 % was used as a target. The glass substrates were ultrasonically cleaned first in acetone and then in alcohol for 15 min before being placed into the deposition chamber. And the distance between the substrate and the target was around 50 mm. The base pressure for the system was 10^{-4} Pa. High-purity argon and oxygen was used as the sputtering and reactive gas, respectively. During depositions, the O_2:Ar ratio was kept as 3:1 and the pressure of the gas mixture was set to 0.7 Pa. By keeping all the other sputtering parameters constant, ZnO thin film samples were deposited at different substrate temperatures (100, 150, 200 ℃) at the constant

RF power of 90 W, and also by varying the RF powers (40, 60, 90 W) at the constant substrate temperature of 200 ℃. The samples are labeled accordingly as $Z_{100\text{-}90}$, $Z_{150\text{-}90}$, $Z_{200\text{-}90}$, $Z_{200\text{-}40}$, and $Z_{200\text{-}60}$.

The crystal structures of all the films were examined by X-ray diffraction (XRD, Rigaku DMAX/VB with Cu Kα $\lambda = 0.154\text{nm}$). The surface morphology and roughness for samples $Z_{100\text{-}90}$, $Z_{200\text{-}90}$, and $Z_{200\text{-}60}$ at the initial stage (after 5 s of sputtering) and that at the final stage (after 45 min of sputtering) were examined with atomic force microscopy (AFM, AJ-Ⅲ). Their optical absorption spectra were recorded by a UV-VIS-NIR spectrophotometer (CARY-500) within the wave-length range of 300 nm to 700 nm.

3. Results and discussion

3.1 Grain growth behavior and surface morphology evolution

Fig. 1(a)-(f) show the variation of surface morphology of the ZnO thin films prepared for the deposition duration of 5 s and 45 min under different sputtering conditions. The root mean square (RMS) roughness R_q and average roughness R_a of a surface were calculated from the integral of the height profile following equation: $R_q = \sqrt{\frac{1}{N}\sum_{n=1}^{N} r_n^2}$ and $R_a = \frac{1}{N}\sum_{n=1}^{N} r_n$, respectively. Here, N is the number of data and r_n is the surface height in the nth data point. The surface RMS and average roughness of the above ZnO thin films are directly determined from the AFM and collected in Table 1.

As shown in Fig.1, all the ZnO thin films deposited by RF reactive magnetron sputtering possess the "island" structure, the grain size of which could be qualitatively analyzed and compared. By comparing Fig. 1 (a), (b), (c), we can find that for the deposition of 5s, the films exhibit the island growth and possess the fine grain structure. Moreover, the grain sizes of sample $Z_{200\text{-}90}$ (Fig. 1 (a)) and sample $Z_{100\text{-}90}$ (Fig. 1 (c)) are about the same and are larger than the size of sample $Z_{200\text{-}60}$ (Fig. 1(b)). It is interesting to note that at the initial deposition stage (after 5s of deposition) the grain size and surface roughness of the films depend mainly on RF power (see Fig. 1 (a), (b), (c), and Table 1), whereas at the final deposition stage (after 45 min of deposition), they depend largely on the substrate temperature (see Fig. 1 (d), (e), (f), and Table 1). An increase of the RF power will most likely increase the bombardment of ions and the average energy of the reactive species, and consequently enhance the reaction rate of Zn and O. Therefore, at the beginning of the sputtering, the higher RF power led both to higher deposition rate and nucleation rate and to the formation of relatively large ZnO grains, while the variation in substrate temperature did not significantly change the grain size. The film deposited at RF power of 60 W ($Z_{200\text{-}60}$) showed the smallest grain size in comparison with the films deposited at 90 W ($Z_{200\text{-}90}$ and $Z_{100\text{-}90}$). At the same time, the surface RMS roughness R_q and average roughness R_a of initial deposited films also increase with increasing RF power, and shows 1.10 and 0.81, 1.36 and 0.98, and 1.86 and 1.12nm for $Z_{200\text{-}60}$, $Z_{100\text{-}90}$, and $Z_{200\text{-}90}$, respectively. Apparently, the surface roughness is closely related to the grain size: the smaller the grain size, the lower the roughness.

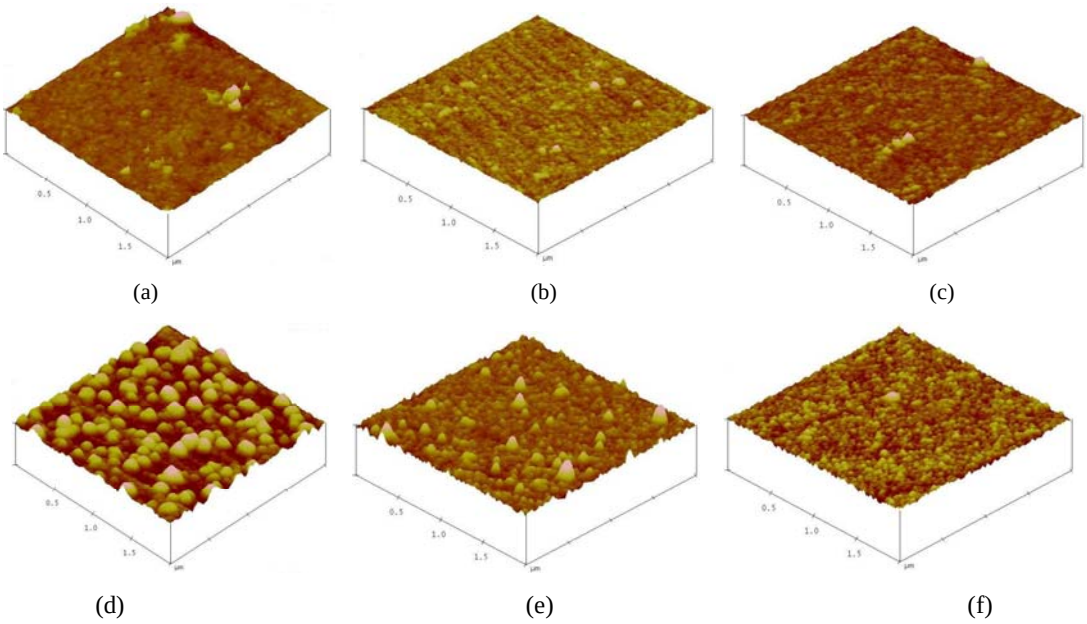

Fig. 1. AFM images of ZnO thin films at initial (5 s) and final (45 min) stages of deposition: (a) 5 s and (d) 45 min for $Z_{200\text{-}90}$; (b) 5 s and (e) 45 min for $Z_{200\text{-}60}$; and (c) 5 s and (f) 45 min for $Z_{100\text{-}90}$.

Table 1. The surface RMS roughness R_q and average roughness R_a of the ZnO thin films corresponding to that shown in Fig.1 (a)-(f).

Sample	$Z_{200\text{-}90}$ (a)-5s	$Z_{200\text{-}90}$ (d)-45 min	$Z_{200\text{-}60}$ (b)-5s	$Z_{200\text{-}60}$ (e)-45 min	$Z_{100\text{-}90}$ (c)-5s	$Z_{100\text{-}90}$ (f)-45 min
R_q (nm)	1.86	18.01	1.10	3.97	1.36	2.16
R_a (nm)	1.12	14.81	0.81	2.63	0.98	1.70

With the increasing sputtering time, large islands are formed as small grains agglomerate. A higher substrate temperature can supply more energy for the ZnO grains deposited on the substrate and thus enhance their surface mobility and the growth rate. Therefore, in comparison with the RF power, substrate temperature affects more on the final surface structure of the growing films. After deposition for 45 min, larger islands (~150-200 nm) start to form among the smaller clusters preferring a spherical top shape in the film deposited at substrate temperature of 200 ℃ and RF power of 90 W ($Z_{200\text{-}90}$), while the film $Z_{200\text{-}60}$ showed a relatively dense structure and smaller average grain size and also possessed a few large islands (~100 nm). Meanwhile, the film deposited at the substrate temperature of 100 ℃ and the RF power of 90 W ($Z_{100\text{-}90}$) exhibited a smoother uniform surface and a denser structure with a smallest average size and a lowest surface roughness of R_q 2.16 nm and R_a 1.70 nm among these samples.

3.2 Structural properties

Fig. 2 shows the XRD patterns of the ZnO films deposited for 45 min at different substrate temperatures (100, 150, and 200 ℃) with a constant RF power of 90 W as well as at the constant substrate temperature of 200 ℃ but with different RF powers (40, 60, 90 W). The XRD spectra revealed that all films deposited at different conditions exhibited polycrystalline nature with the diffraction peaks corresponding to the (002), (100), (101), and (110) reflections of hexagonal wurtzite ZnO. The ZnO film (sample $Z_{200\text{-}60}$) deposited at 200 ℃ and 60 W has the strongest (002) peak intensity, indicating that the film has a very strong orientation along the c-axis and the crystallinity of the film was significantly improved.

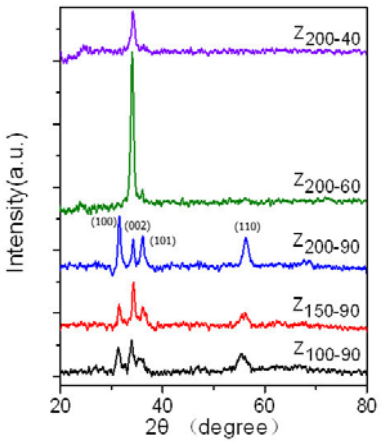

Fig. 2. XRD patterns of the ZnO films prepared at different substrate temperatures and RF powers.

The lattice constant, position, full width at half maximum (FWHM), and intensity of (002) peaks from the XRD patterns of different samples are listed in Table 2. The average grain dimension D can be calculated using the Sherrer formula: $D = 0.9\lambda / B\cos\theta$, where λ, θ and B are the x-ray wavelength, the Bragg diffraction angle, and the FWHM of the (002) peak, respectively. The film stress (σ_f) parallel to the film surface has been given by the following numerical relation: $\sigma_f = -233(C - C_0)/C_0$ [16,17], here C and C_o are the lattice constants of ZnO films from XRD and bulk ZnO, respectively. The negative or positive values of σ_f represent the compressive or tensile stresses acting in the film plane, respectively. The calculated parameters discussed above for different samples are collected in Table 2. The relative peak intensity $I_{002}/\sum I_{ijk}$, average grain size (D), and absolute value (σ) of the stresses σ_f as a function of substrate temperature (××~T) at the constant RF power of 90 W and as a function of RF power (××~P) at the constant substrate temperature of 200 ℃ are plotted in Fig.3 (a), (b), and (c), respectively.

Table 2. The data evaluated from XRD patterns of the ZnO films

Sample	$Z_{100\text{-}90}$	$Z_{150\text{-}90}$	$Z_{200\text{-}90}$	$Z_{200\text{-}60}$	$Z_{200\text{-}40}$
2θ(deg)	34.02	34.26	34.36	34.24	34.20
C (nm)	0.5266	0.5230	0.5215	0.5233	0.5239
FWHM(deg)	1.234	0.618	0.580	0.799	0.944
Intensity	533	795	507	2783	796
$I_{002}/\sum I_{iik}$	0.36	0.42	0.21	0.85	0.60
D (nm)	6.65	13.30	14.17	10.29	8.71
σ_f (Gpa)	-2.685	-1.074	-0.448	-1.208	-1.477

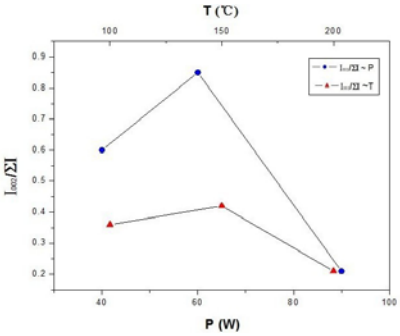

(a)

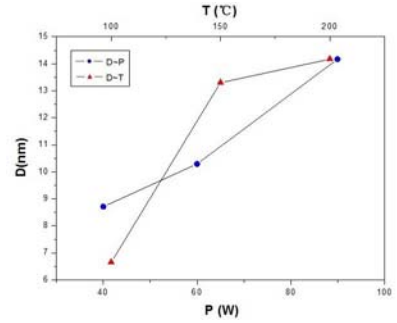

(b)

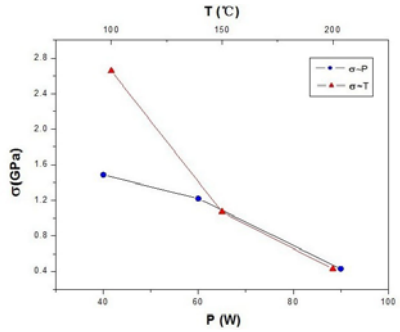

(c)

Fig. 3. Variations of (a) relative peak intensity, (b) grain dimension, and (c) stress with substrate temperature (~T) at 90 W and RF power (~P) at 200 ℃.

As shown in Fig 3(a), $I_{002}/\sum I_{ijk}$ increases significantly with the increase of the RF power from 40 W to 60 W, indicating an enhancement in crystalline of the ZnO films. However, as the RF power is further increased up to 90 W, $I_{002}/\sum I_{ijk}$ decreases sharply, and the XRD pattern (see Fig.2) exhibited a (100) diffraction peak with a higher intensity. The investigations by Lin et al[18] and Flickyngerova et al[19] also indicated similar results in their ZnO:Al thin films. It may be explained that a higher RF power (bigger than 90 W in this study) would lead to a more intensive ion bombardment and a faster deposition rate, which results in an increase of the defects and thereby gives rise to the development of a (100) texture and the degradation of the (002) preferred orientation in the growth of the films. Meanwhile, $I_{002}/\sum I_{ijk}$ of the ZnO films, deposited at different substrate temperature with the RF power of 90 W, varies only slightly with substrate temperature.

It can be seen from Fig. 3 (b), and (c), and Table 2 that the residual stress in all investigated ZnO thin films corresponds to a compressive state. With the increase of the RF power or the substrate temperature, the grain size increases and the compressive stress reduces. Furthermore, the trend of the decrease in the compressive stress with the increase of the RF power or the substrate temperature is identical with that of the increase in the grain size (see Fig.3(b) and (c)). We believe that the enhancement of RF power and substrate temperature will lead to the increase of the deposition rate and the growth rate, respectively, resulting in the increase in the grain size. Larger grain size might result in an effective release of the compressive stress due to a grain boundary relaxation [20].

Gupta and Mansingh [21] attributed the presence of the stress in ZnO films to oxygen interstitial defects. In our work, all the films were prepared in oxygen-sufficient atmosphere with the O_2:Ar ratio of 3:1 and it is possible that oxygen interstitials form in the films. Thus, the intrinsic stress in the deposition ZnO films should be attributed to the presence of oxygen interstitials, which has an expansive effect on the crystal lattice along c-axis and results in a compressive stress [22]. Therefore, with the increase of RF power and substrate temperature, the amount and energy of Zn species from a metal target are enhanced and the reaction between Zinc and oxygen becomes complete, which might cause a decrease in interstitial oxygen and accordingly lead to a decrease of compressive stress in the films.

In addition, comparison with the RF power, the substrate temperature has more evident influence on the larger grain growth. Moreover, the major grain growth yields a significant increase in the surface roughness (see Fig.1 (d) and Table 1), which also leads to a lower (002) peak intensity and development of (100) texture. The ZnO film (sample $Z_{200\text{-}90}$) deposited at the RF power of 90 W and substrate temperature of 200 ℃ showed the smallest stress and the largest grain size, and the relative peak intensity $I_{002}/\sum I_{ijk}$ of the (002) plane decreased significantly (see Fig. 3). So considering the degree of

(002) preferential orientation and the smoother surface structure, we suggest that a control of lower RF power and a higher substrate temperature is needed. The RF power of 60 W and the substrate temperature of 200 ℃ are the optimal deposition parameters for growing ZnO thin films in the present experiment.

3.3 Optical properties

Fig. 4(a) shows the absorption spectra in the range of 300-700 nm of sample $Z_{200\text{-}90}$, $Z_{100\text{-}90}$, and $Z_{200\text{-}60}$. A shoulder followed by a peak around the wavelength 360 nm is observed in the spectra for sample $Z_{200\text{-}90}$, which is contributed by the ZnO exciton [23,24]. The reduction of both substrate temperature and RF power results in a significant decrease in the intensity of the excitonic peak (for samples $Z_{200\text{-}60}$ and $Z_{100\text{-}90}$). The influence of the substrate temperature on the ZnO excitonic peak intensity is larger than that of RF power, in accordance with their corresponding effect on the grain size as already mentioned above.

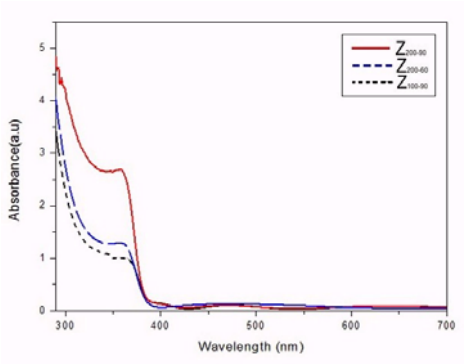

(a)

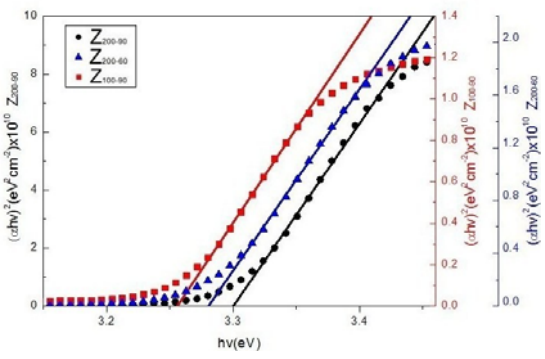

(b)

Fig. 4. Optical properties of ZnO thin films: (a) absorption spectra and (b) plots of $(\alpha h\nu)^2$ *vs* $h\nu$.

The plots of $(\alpha h\nu)^2$ vs $h\nu$ are shown in Fig. 4 (b). Where, α represents the absorption coefficient and $h\nu$ is the incident photon energy. According to the following relation [25]: $(\alpha h\nu)^2 = A(h\nu - E_g)$, the optical band gap energy E_g of the films was estimated by extrapolation of the linear portion of $(\alpha h\nu)^2$ vs $h\nu$ curve. The optical band gaps of sample $Z_{100\text{-}90}$, $Z_{200\text{-}60}$, and $Z_{200\text{-}90}$ are about 3.26 eV, 3.28 eV, and 3.30 eV, respectively, and they increase with the increase in the substrate temperature and RF power. This broadening in the optical band gaps can be attributed to the increase in the crystallite grain size and the relaxation of the compressive stress in the ZnO films, which is different from the results reported by Kumar et al [23], where the optical band gaps of ZnO films has been found to decrease with the increase in the substrate temperature and crystallite size, and which has been attributed to the decrease in the stress. We suggest that the different effects observed in the thin films by varying the substrate temperature and RF power is probably due to the difference in the origin of stress in the films. Kumar et al [23] deposited all ZnO films using a sintered ZnO target for the sputtering in oxygen deficient atmosphere, which indicates the presence of extra Zn in the deposited ZnO films. Thus, the intrinsic stress in the films could be originated from the presence of Zn interstitials. With the increase in the substrate temperature, the intrinsic compressive stress decreases in the films, which corresponds to the decrease in Zn interstitials, and so the value of optical band gap decreases. In the present experiment we prepared all the films by reaction deposition using Zinc as the sputtering target in oxygen sufficient atmosphere. There exists the possibility of the formation of oxygen interstitial defects, which leads to the presence of compressive stress in the ZnO films. So the relaxation of the compressive stress corresponds to the decrease in the oxygen interstitials, which probably give rise to the observed increase in E_g value of ZnO thin films. Thus, in the present case, with increasing substrate temperature and RF power, the larger the crystal grain size, the less the compressive stress, the stronger the ZnO excitonic peak, and the broader the optical band gap. Further work is needed in order to elucidate the effect of these factors on optical band gap.

4. Conclusion

The effect of substrate temperature and RF power on the structural and optical properties of ZnO thin films deposited by RF reactive magnetron sputtering has been investigated. The behavior of the grain growth and the evolution of the surface morphology in the films at the initial and final sputtering stages are also observed. For the films deposited for 5 s, the ZnO grain size and the surface roughness were mainly dependent on the RF power and they increase with increasing RF power as the results of high deposition rate and nucleation rate. After deposition for 45 min, the grain size and surface roughness of the ZnO films were significantly influenced by the substrate temperature, and they increase with increasing substrate temperature as the results of high surface mobility and growth rate. In the present experiment, the residual stress in all the ZnO films deposited exhibits a compressive state. With the increase of both substrate temperature and RF power, the crystallite size increases and the compressive stress decreases. Higher RF power and larger grain growth can also induce a high defect density and result in a rougher surface, respectively, which lead to lower intensity of (002) peak. Therefore, the control of the relatively low RF power and high substrate temperature is beneficial to the increase in the (002) preferential orientation. The intensity of ZnO excitonic peak and the optical band gap (E_g) increase with increasing both RF power and substrate temperature, which has been attributed to the increase in the grain size and the relaxation of the compressive stress in the films.

References

[1] M. K. Chong, A. P. Abiyasa, K. Pita, S. F. Yu, Appl. Phys. Lett. **93**, 151105(2008).
[2] G.. T. Du, Y. G. Cui, X. C. Xia, X. P. Li, H. C. Zhu, B. L. Zhang, Y. T. Zhang, Y. Ma, Appl. Phys. Lett. **90**, 243504 (2007).
[3] H. Sato, T. Minami, Y. Tamura, S. Takate, T. Mouri, N. Ogawa, Thin Solid Films, **246**, 86 (1994).
[4] Y. Yoshino, T. Makino, Y. Katayama, T. Hata, Vacuum. **59**, 538 (2000).
[5] C. M. Nahm, Mater Lett. **62**, 4440 (2008).
[6] J. Q. Xu, Y. A. Shun, Q. G. Pan, J. H. Qin, Sensors and Actuators B. **66**, 161(2000).
[7] J. Hu, R. G. Gordon, J. Appl. Phys. **72**, 5381 (1992).
[8] Y. W. Heo, D. P. Norton, S. J. Pearton, J. Appl. Phys. **98**, 073502.1(2005).
[9] J. H. Choi, H. Tabata, T. Kawai, J. Cryst. Growth, **226**, 493(2001).
[10] Y. S. Kim, W. P. Tai, S. J. Shu, Thin Solid Films. **491**, 153(2005).
[11] K. Ellmer, J. Phys. D. **32**, R17 (2000).
[12] T. B. Hur, Y. H. Hwang, H. K. Kim, I. J. Lee, J. Appl. Phys. **99**, 064308 (2006).
[13] K. U. Sim, S. W. Shin, A. V. Moholkar, J. H. Yun, J. H. Moon, J. H. Kim, Current Applied Physics. **10**, S463(2010).
[14] W. Gao, Z. W. Li, Ceramics International. **30**, 1155 (2004).
[15] Y. Y. Liu, Y. L. Zang, G. X. Wei, J. Li, X. L. Fan, C. F. Chen, Mater Lett. **63**, 2597 (2009).
[16] H. C. Ong, A. X. E. Zhu, G. T. Du, Appl. Phys. Lett. **80**, 941 (2002).
[17] M. K. Puchert, P. Y. Timbrell, R. N. Lamb, J. Vac. Sci. Technol A. **14**, 2220 (1996).
[18] Y. C. Lin, M. Z. Chen, C. C. Kuo, W. T. Yen, Colloids and Surfaces A: Physicochem. Eng. Aspects. **337**, 52 (2009).
[19] S. Flickyngerova, K. Shtereva, V. Stenova, D. Hasko, I. Novotny, V. Tvakozek, P. Sutta, E. Varrinsky, Applied Surface Science. **254**, 3643 (2008).
[20] L. Parfitt, M. Goldiner, J. W. Jones, G.. S. Was, J. Appl. Phys. **77**, 3029 (1995).
[21] V. Gupta, A. Mansingh, J Appl Phys. **80**, 1063 (1996).
[22] L. W. Wang, L. J. Meng, V. Teixeira, S. G. Song, Z. Xu, X. R. Xu, Thin Solid Films. **517**, 3721 (2009).
[23] R. Kumar, N. Khare, V. Kmar, G. L. Bhalla, Applied Surface Science. **254**, 6509 (2008).
[24] J. L. Chen, R. Mu, A. Ueda, M. H. Wee, Y. S. Tung, Z. Gu, D. D. Henderson, J Vac. Sci. Technol A.**16**, 1409 (1998).
[25] N. Serpone, D. Lawless, R. Khairutdinov, J Phys. Chem. **99**, 16646 (1995).

*Corresponding author: luhui@ecust.edu.cn